NEOPLASIA
www.neoplasia.com

Volume 16 Number 2 February 2014 pp. 147–157 147

BMX Acts Downstream of PI3K to Promote Colorectal Cancer Cell Survival and Pathway Inhibition Sensitizes to the BH3 Mimetic ABT-737[1,2]

Danielle S. Potter*, Paul Kelly*, Olive Denneny*, Veronique Juvin†, Len R. Stephens†, Caroline Dive*,3 and Christopher J. Morrow*,3

*Clinical and Experimental Pharmacology Group, Cancer Research UK Manchester Institute, University of Manchester, Manchester, United Kingdom; †Inositide Laboratory, Babraham Institute, Babraham Research Campus, Cambridge, United Kingdom

Abstract

Evasion of apoptosis is a hallmark of cancer, and reversing this process by inhibition of survival signaling pathways is a potential therapeutic strategy. Phosphoinositide 3-kinase (PI3K) signaling can promote cell survival and is upregulated in solid tumor types, including colorectal cancer (CRC), although these effects are context dependent. The role of PI3K in tumorigenesis combined with their amenability to specific inhibition makes them attractive drug targets. However, we observed that inhibition of PI3K in HCT116, DLD-1, and SW620 CRC cells did not induce apoptotic cell death. Moreover, these cells were relatively resistant to the Bcl-2 homology domain 3 (BH3) mimetic ABT-737, which directly targets the Bcl-2 family of apoptosis regulators. To test the hypothesis that PI3K inhibition lowers the apoptotic threshold without causing apoptosis *per se*, PI3K inhibitors were combined with ABT-737. PI3K inhibition enhanced ABT-737–induced apoptosis by 2.3- to 4.5-fold and reduced expression levels of MCL-1, the resistance biomarker for ABT-737. PI3K inhibition enhanced ABT-737–induced apoptosis a further 1.4- to 2.4-fold in CRC cells with small interfering RNA–depleted MCL-1, indicative of additional sensitizing mechanisms. The observation that ABT-737–induced apoptosis was unaffected by inhibition of PI3K downstream effectors AKT and mTOR, implicated a novel PI3K-dependant pathway. To elucidate this, an RNA interference (RNAi) screen of potential downstream effectors of PI3K signaling was conducted, which demonstrated that knockdown of the TEC kinase BMX sensitized to ABT-737. This suggests that BMX is an antiapoptotic downstream effector of PI3K, independent of AKT.

Neoplasia (2014) 16, 147–157

Introduction

Single-agent treatments rarely prove sufficient for cancer cure. This is in part due to a variety of innate or acquired, drug-specific, or pleiotropic drug resistance mechanism(s), one of which is suppression of drug-induced cell death. Consequently, there is considerable motivation to overcome drug resistance mechanisms by identifying rational combinations of molecular targeted drugs. To aid this, the US Food and Drug Administration (FDA) is considering early-phase drug combination trials without the necessity for prior single-agent approval [1]. Historically, choice of drug combinations is predicated

Abbreviations: CRC, colorectal cancer; PI3K, phosphoinositide 3-kinase; PtdIns(3,4,5)P_3, phosphatidylinositol-3,4,5-triphosphate; PH, pleckstrin homology; siRNA, small interfering RNA; SRB, sulforhodamine B

Address all correspondence to: Christopher J. Morrow, PhD, or Caroline Dive, PhD, Cancer Research UK Manchester Institute, University of Manchester, Wilmslow Road, Manchester, M20 4BX, United Kingdom. E-mail: christopher.morrow@cruk.manchester.ac.uk, caroline.dive@cruk.manchester.ac.uk

[1]This work was supported by Cancer Research UK (CR-UK) core funding to the CR-UK Manchester Institute (grant No. C147/A12328). O.D. was supported through funding from the Cancer Research UK Experimental Cancer Medicine Centre grant to the Manchester Cancer Research Centre.

[2]This article refers to supplementary materials, which are designated by Tables W1 to W8 and Figures W1 to W9 and are available online at www.neoplasia.com.

[3]These authors contributed equally to this work.

Received 23 July 2013; Revised 12 December 2013; Accepted 17 January 2014

DOI 10.1593/neo.131376

on nonoverlapping drug toxicities; however, the concept of targeting multiple different hallmarks of cancer is an emerging approach [2]. Two such hallmarks are sustained inappropriate proliferative signaling and suppression of apoptotic cell death [2]. Molecular features that contribute to these hallmarks in several human tumors, including colorectal cancer (CRC), are aberrations in the phosphoinositide 3-kinase (PI3K) signaling pathway and up-regulation of antiapoptotic Bcl-2 family proteins. This study examines the combined effect of inhibiting PI3K signaling and interrupting the protein-protein interactions between proapoptotic and antiapoptotic members of the Bcl-2 family in CRC cells.

PI3K phosphorylates the 3-hydroxy group of phosphatidylinositol lipid rings to generate a secondary messenger that is implicated in many intracellular signaling pathways. The most studied are the class I PI3Ks, which phosphorylate phosphatidylinositol-4,5-bisphosphate generating phosphatidylinositol-3,4,5-triphosphate [PtdIns(3,4,5)P_3] [3]. PtdIns(3,4,5)P_3 is a docking site for a number of proteins that contain PtdIns(3,4,5)P_3-binding motifs such as pleckstrin homology (PH) domains, frequently leading to activation of the docked protein. The best characterized effectors of the pathway are phosphoinositide-dependent kinase 1 (PDK1) and AKT (AKA protein kinase B). PDK1 and AKT bind to PtdIns(3,4,5)P_3, allowing PDK1 to phosphorylate and activate AKT [4]. Activation of AKT has multiple cell fate outcomes including increased cell survival, sustained cell proliferation, and enhanced cell migration, all of which have potential to promote oncogenesis [5]. Aberrant PI3K signaling is implicated in many cancer types. For example, loss of the PI3K antagonistic phosphatase PTEN and activating mutations in *PIK3CA*, the gene encoding the catalytic PI3K subunit p110α, are among the most common genetic aberrations in cancer [6]. Consequently, the PI3K signaling pathway is a major focus of drug discovery programs, with multiple small-molecule inhibitors targeting PI3K, AKT, and other PI3K pathway components undergoing clinical trials [6]. Multiple lines of preclinical evidence suggest that PI3K signaling acts to suppress apoptosis through mechanisms including the modulation of Bcl-2 family proteins that control the release of potent apoptogens from mitochondria [5]. However, despite this body of evidence, apoptosis is not induced in many cancer cell lines after specific inhibition of PI3K pathway signaling [7,8]. Furthermore, emerging evidence shows that, whereas in some cell types, combining PI3K inhibition with conventional chemotherapeutic agents induces apoptosis [9,10], this is not the case with CRC cells [7], a disease where aberrant PI3K activation is common.

Drug development efforts to disrupt interactions between proapoptotic and antiapoptotic proteins of the Bcl-2 family yielded the Bcl-2 homology domain 3 (BH3) mimetic class of drugs [11]. The "poster-child" BH3 mimetic ABT-737 and its related clinical candidate navitoclax readily induce apoptosis in small cell lung cancer *in vitro* and *in vivo* as a single agent [12] and kill lymphoma cell lines and primary lymphoma cells *ex vivo* [12,13], and navitoclax has demonstrated promising results in a phase I clinical trial in patients with chronic lymphocytic leukemia [14]. However, in several cancer cell types, including CRC, ABT-737 treatment alone does not induce apoptosis at clinically relevant concentrations [15]. In a broad range of cancer cell types, ABT-737 acts synergistically with a variety of conventional and novel chemotherapeutic agents [16], including agents that target the PI3K pathway [17,18]. This suggests that a lowering of the apoptotic threshold by ABT-737 facilitates the coupling of drug-induced damage and/or the interruption of survival signaling events to the commitment to apoptotic cell death. Therefore, the hypothesis tested in this study was that PI3K pathway ablation using small-molecule inhibitors could "prime" CRC cells for apoptosis but that cell death would only be realized if the actions of antiapoptotic Bcl-2 family proteins were negated by a BH3 mimetic.

Materials and Methods

Cell Culture and Drugs

HCT116, DLD-1 [American Type Culture Collection (ATCC), Manassas, VA], and isogenic pairs of HCT116 and DLD-1 expressing only wild-type or mutant PIK3CA (a kind gift from B. Vogelstein) were cultured in McCoy's 5A media (Life Technologies, Inc, Paisley, United Kingdom) supplemented with 10% FBS (BioWest, Nuaillé, France). SW620 (ATCC) were cultured in Dulbecco's modified Eagle's medium supplemented with 10% FBS and glutamine (Life Technologies, Inc). All cells were maintained in a humidified atmosphere at 37°C and 5% CO_2. Cell lines were authenticated using the AmpFlSTR system (Applied Biosystems, Paisley, United Kingdom) during the study. ABT-737 (a kind gift from AbbVie, Chicago, IL), PI-103, rapamycin, Akti1/2, KU-0063794 (Merck, Nottingham, United Kingdom), GDC-0941, MK-2206, and PCI-32765 (Selleck Chemicals, Houston, TX) were all dissolved to 10 mM in DMSO (Sigma, Dorset, United Kingdom) and stored as single use aliquots at −20°C/−80°C (Figure W1).

Concentration Response

Cells were seeded into 96-well plates. After 24 hours, cells were treated with the indicated concentration of drug(s) and cultured for a further 72 hours in the presence of drug(s). Plates were stained with sulforhodamine B (SRB) and processed as previously described [7] to give an indication of cellular biomass. To determine logGI_{50}, log drug concentration was plotted against raw absorbance, and nonlinear curve fit analysis was performed (GraphPad Prism; GraphPad Software, La Jolla, CA). Statistical analysis was carried out on three independent logGI_{50} readings and transformed to growth inhibition 50 (GI_{50}) for presentation. For display purposes only, drug concentration (log scale) has been plotted against normalized absorbance.

Western Blot Analysis

Cell lysis and Western blot analysis were carried out as previously described [7]. The following primary antibodies were used: rabbit anti-pS473AKT (No. 4058), rabbit anti-AKT (No. 9297), rabbit anti-pT246 40-kDa proline-rich AKT substrate (PRAS40) (No. 2997), rabbit anti-PRAS40 (No. 2691), pS240/244S6 (No. 4838), rabbit anti-S6 (No. 2217), rabbit anti–cleaved caspase 3 (No. 9661), rabbit anti-PARP (No. 9542), rabbit anti-Bax (No. 2774; all from Cell Signaling Technology, Danvers, MA), mouse anti–Bcl-2 (M0887; Dako, Glostrup, Denmark), rabbit anti–BCL-XL (No. 610211; Becton Dickinson, Oxford, United Kingdom), mouse anti-human MCL-1 (No. 559027; Becton Dickenson), rabbit anti–MCL-1 (sc819; Santa Cruz Biotechnology, Inc, Dallas, TX), rabbit anti-Bad (AF819; R&D Systems, Minneapolis, MN), rabbit anti-Bim (No. 202000; Merck), mouse anti-Bak (AM03; Merck), mouse anti–α-tubulin (CP06; Merck), and mouse anti-GAPDH (G9545; Sigma).

Measurement of Apoptosis

Annexin V/7-aminoactinomycin D (7AAD) flow cytometry was performed as previously described [7]. For assessment of Bak conformational change, cells were cultured in a 96-well plate and

treated with the indicated drug(s) for 24 hours. Cells were fixed with 1% formaldehyde and sent to Imagen Biotech (Cheshire, United Kingdom) where immunofluorescent staining for conformationally changed Bak and high-content analysis were carried out using proprietary protocols using Bak conformation–specific antibodies. Real-time assessment of cells with activated Caspase 3/7 was carried out using the CellPlayer apoptosis Caspase 3/7 reagent (Essen BioScience, Ann Arbor, MI) following manufacturer's recommendations. Cells were placed in an IncuCyte (Essen BioScience) and imaged every 2 hours. The number of fluorescent cells per field of view was determined using IncuCyte software (Essen BioScience) following manufacturer's recommendations.

RNA Interference (RNAi)

siRNA SMARTpools or individual oligos (Thermo Scientific, Leicestershire, United Kingdom) were transfected into SW620 or HCT116 cells using DharmaFECT 2 (Thermo Scientific) according to manufacturer's instructions. For the small interfering RNA (siRNA) library screen, cells were reverse transfected with 5 pmol of siRNA in 6 wells of a 96-well plate per SMARTpool and left for 48 hours, 3 wells were treated with 4 μM ABT-737, and 3 wells were treated with DMSO equivalent. For other siRNA experiments, siRNA were transfected in six-well plates, reseeded into appropriate culture vessels 24 hours later, and drug treated after another 24 hours. Calculation of robust z score is described in Supplemental Materials and Methods section.

Real-Time Quantitative Polymerase Chain Reaction

Quantitative polymerase chain reaction (qPCR) was carried out as previously described [19]. Assays for *bone marrow tyrosine kinase* gene in chromosome X protein (*BMX*), SOS1, and SGK1 were designed with the Roche (West Sussex, United Kingdom) Universal ProbeLibrary Assay Design Center.

Statistical Analysis

Unpaired, two-tailed t tests were performed in Excel (Microsoft, Redmond, WA) to determine significance. $P < .05$ was considered significant.

Results

PI-103 Sensitized CRC Cell Lines to ABT-737

The purpose of this study was to investigate the effect of combining ABT-737 with PI3K pathway inhibitors in CRC cell lines. The lines used were HCT116 and DLD-1, which carry oncogenic activating mutations in *PIK3CA*, and SW620 cells that are wild type for *PIK3CA* [20]. All three cell lines also harbor mutant *KRAS* (www.sanger.ac.uk/genetics/CGP/cosmic/), which can activate the PI3K signaling pathway [4]. All cell lines were responsive to the PI3K/mammalian target of rapamycin (mTOR) inhibitor PI-103 in the SRB assay, which measures cellular biomass, with GI_{50} values of 288 nM in HCT116 [95% confidence interval (CI) = 255-325 nM], 184 nM in DLD-1 (95% CI = 132-256 nM), and 636 nM in SW620 cells (95% CI = 508-797 nM) (Figure W2*A*). The phosphorylation of PI3K and/or mTOR effectors AKT, PRAS40, and S6 was inhibited by PI-103 in all cell lines (Figure W2*B*), confirming that PI-103 inhibited PI3K and mTOR. To determine whether PI-103 treatment affected CRC cell sensitivity to ABT-737, HCT116, SW620, and DLD-1 cells were treated concomitantly with PI-103 and/or ABT-737 (Figure 1*A* and Table 1). All cell lines exhibited a concentration-dependent response to ABT-737 alone, and the ABT-737 GI_{50} was reduced significantly in a concentration-dependent manner by PI-103. This is consistent with PI3K inhibition sensitizing CRC cells to ABT-737. The observation that PI-103 increased the sensitivity toward ABT-737 irrespective of *PIK3CA* mutation status suggests that *PIK3CA* mutation is not essential for this effect.

PI-103 Enhanced ABT-737–Induced Apoptosis

The effect of PI-103 on the levels of ABT-737–induced apoptosis was determined by several methods. First, the effect of ABT-737 and/or PI-103 on caspase 3 and PARP cleavage was determined by Western blot analysis (Figure 1*B*). ABT-737 alone induced some caspase 3 and PARP cleavage, whereas PI-103–only treatment had no effect. Combining the two agents increased caspase 3 and PARP cleavage, suggesting that the combination caused more apoptosis than either agent alone. The effect of ABT-737 and PI-103 on the externalization of phosphatidylserine, another classic biomarker of apoptosis, was determined by flow cytometry in HCT116 and SW620 cells (Figure 1*C*). In both cases, neither PI-103 nor ABT-737 alone caused a significant level of apoptosis compared to untreated cells, whereas combining ABT-737 and PI-103 gave significantly more apoptosis than any other condition.

PI3K signaling can promote numerous antiapoptotic mechanisms that act upstream or downstream of cytochrome *c* release from mitochondria, for example, Bad sequestration and caspase 9 inhibition, respectively [21,22]. To determine whether the PI-103–induced ABT-737 sensitization was upstream of cytochrome *c* release, the percentage of HCT116 cells exhibiting the early activating N-terminal conformational change in the multidomain proapoptotic protein Bak [23] was assessed by immunofluorescence. The combination of PI-103 and ABT-737 resulted in a significantly higher proportion of cells with activated Bak than either agent alone (Figure 1*D*). This confirmed that PI-103 sensitized CRC cells to ABT-737–induced apoptosis and that this effect was mediated upstream of cytochrome *c* release.

ABT-737 Sensitization Was Not Solely due to MCL-1 Down-Regulation

There is precedence for PI3K inhibition affecting several Bcl-2 family members including Bad, Bim, Bcl-2, MCL-1, and Bax [5]. When the effect of PI-103 on expression levels of 10 Bcl-2 family members was assessed by Western blot analysis in HCT116 and SW620 cells, the only observed change was a reduction in MCL-1 level (Figure 2*A*). MCL-1 is an established resistance biomarker for ABT-737, due to the poor affinity of ABT-737 for this antiapoptotic Bcl-2 family member [24,25]. Moreover, MCL-1 stability is known to be decreased by PI3K inhibition due to activation of GSK3β [26]. To test the hypothesis that PI-103–induced sensitivity to ABT-737 was solely due to a reduction of MCL-1 levels, MCL-1 was depleted by siRNA (Figure 2*B*), and the effect of PI-103 on ABT-737 sensitivity was reassessed. If the effect of PI3K inhibition on ABT-737 sensitivity is mediated only through MCL-1 down-regulation, treatment with PI-103 should not further sensitize MCL-1–depleted cells to ABT-737. MCL-1 knockdown significantly sensitized both HCT116 and SW620 to ABT-737, reducing the GI_{50} to a similar extent to that in cells transfected with nontargeting siRNA and treated with PI-103

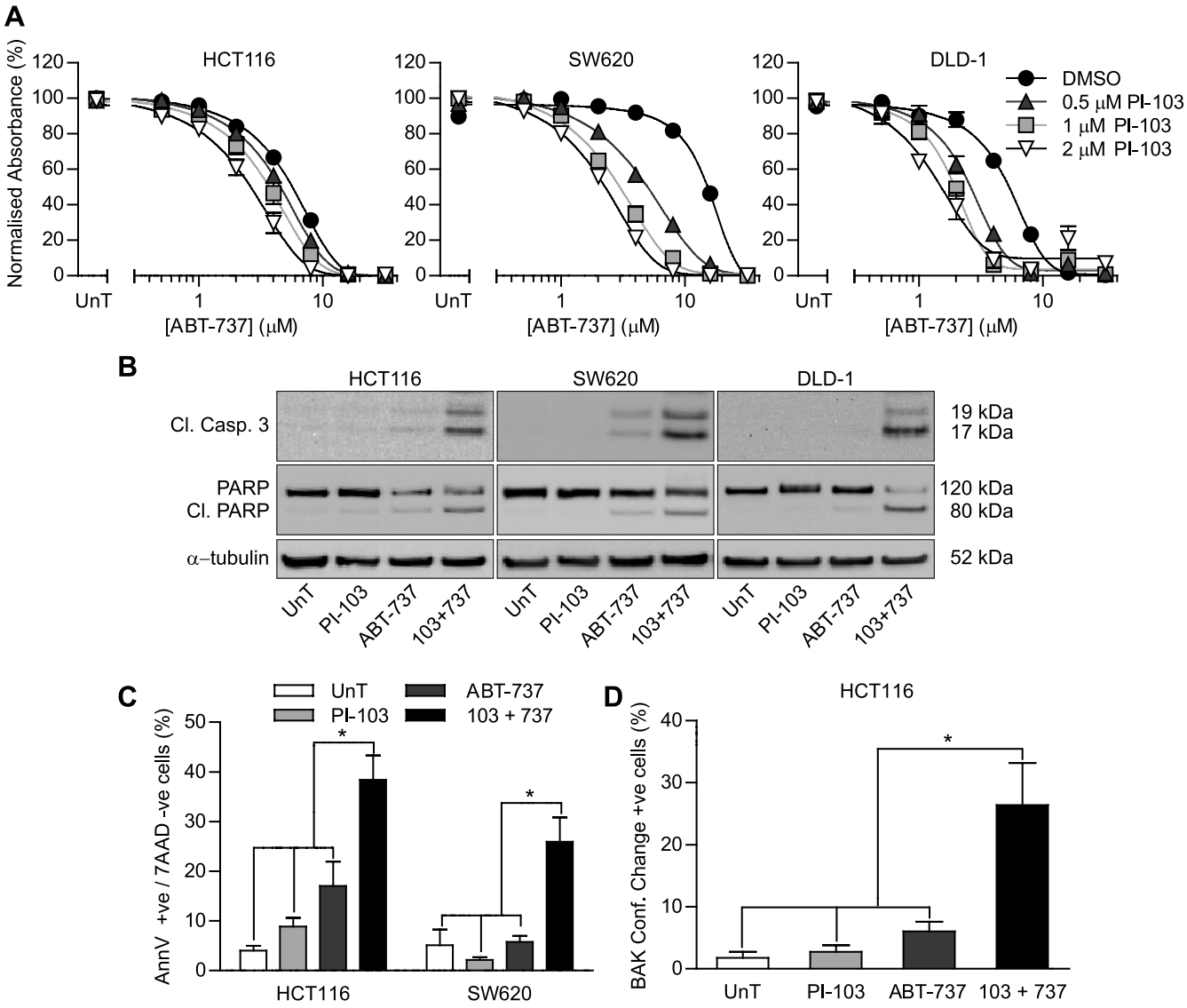

Figure 1. PI-103 sensitized CRC Cell Lines to ABT-737–induced apoptosis. (A) Cells were exposed to DMSO or the indicated concentration of PI-103 and the indicated concentration of ABT-737 for 3 days. Cells were fixed and stained with SRB, and the absorbance relative to untreated (UnT) cells was determined relative to DMSO or PI-103 only–treated cells as appropriate for individual concentration response curves. (B–D) Cells were treated with the indicated combinations of 4 μM ABT-737 (A and B) or 8 μM ABT-737 (C) and 2 μM PI-103 for 24 hours. (A) The level of cleaved caspase 3, full-length PARP, cleaved PARP, and α-tubulin was assessed by Western blot analysis. Results are representative of three independent experiments. (B) Cells were stained with allophycocyanin (APC)-conjugated annexin V and 7AAD, and the percentage of annexin V–positive/7AAD-negative cells was determined by flow cytometry. (C) Cells were fixed and stained for conformationally changed BAK, and the percentage of positive cells was determined by immunofluorescence. All graphs represent the means of three independent experiments carried out in triplicate (A) or duplicate (C and D) ± SEM. *$P < .05$ according to two-tailed unpaired *t* test.

(Figure 2*C* and Table W1). However, PI-103 significantly increased sensitivity to ABT-737 in MCL-1 knockdown cells. To determine whether this additional increase in ABT-737 sensitivity was due to apoptosis, cells were transfected with nontargeting siRNA or MCL-1–specific siRNA, treated with combinations of ABT-737 and/or PI-103, and analyzed by annexin V/7AAD flow cytometry (Figure 2*D*). This confirmed that, in MCL-1–depleted HCT116 and SW620 cells, PI-103 treatment increased ABT-737–induced apoptosis. One experimental caveat is that, whereas MCL-1 was clearly depleted by siRNA, a detectable level remained, and PI-103 could be reducing the MCL-1 levels further (beyond the resolution of the assay). Thus, the increased apoptosis observed could still be MCL-1 dependent. To address this, similar studies were performed in MCL-$1^{-/-}$ mouse embryonic fibroblasts (MEFs). MCL-1 knockout was confirmed (Figure W3*A*), and combining ABT-737 and PI-103 gave a significantly greater decrease in colony formation than either agent alone (Figure W3*B*). Furthermore, the combination gave enhanced cell death in parental and MCL-$1^{-/-}$ MEFs (Figure W3*C*). Although the mechanism of PI-103–induced sensitization to ABT-737 may be different between CRC cell lines and MEFs, this further demonstrates that MCL-1 is not essential for PI-103–induced sensitization. Taken together, these data suggest that, although reduced levels of MCL-1 in PI-103–treated cells caused

Table 1. Effect of PI-103 Treatment on ABT-737 GI_{50}.

Cell Line	Treatment	ABT-737 GI_{50} (μM ± 95% CI)	Significance*
HCT116	DMSO	5.80 (5.16-6.52)	
	0.5 μM PI-103	4.70 (4.30-5.15)	0.0495
	1 μM PI-103	4.39 (3.78-5.09)	0.0439
	2 μM PI-103	3.11 (2.26-4.29)	0.0231
SW620	DMSO	15.5 (14.2-16.8)	
	0.5 μM PI-103	5.07 (3.75-6.84)	0.0022
	1 μM PI-103	2.88 (2.14-3.88)	0.0004
	2 μM PI-103	2.22 (1.86-2.66)	<0.0001
DLD-1	DMSO	5.35 (5.15-5.55)	
	0.5 μM PI-103	2.44 (2.19-2.71)	0.0002
	1 μM PI-103	1.82 (1.60-2.07)	0.0001
	2 μM PI-103	1.36 (0.99-1.87)	0.0011

*Two-tailed unpaired *t* test *versus* DMSO-treated GI_{50} for same cell line.

sensitization to ABT-737, there are additional MCL-1–independent events that influence the response to ABT-737.

ABT-737 Sensitization Was due to Inhibition of PI3K but Not AKT or mTOR

PI-103 is a dual PI3K/mTOR inhibitor; therefore, it was investigated whether the effect of PI-103 on ABT-737 sensitivity was due to PI3K inhibition, mTOR inhibition, and/or off-target effects. To assess this, PI3K signaling was genetically altered. This was achieved using HCT116 and DLD-1 cells, both of which normally express one mutant and one wild-type *PIK3CA* allele (labeled Parental). In the isogenic cell lines, one allele had been silenced by insertion of an adeno-associated virus (AAV)–targeting system into exon 1 of either the wild-type or mutant *PIK3CA* [27]. If the AAV inserted into the wild-type *PIK3CA* allele, only the mutant protein was expressed, resulting in higher PI3K activity compared to parental cells (labeled Mutant). Conversely, if the AAV inserted into the mutant *PIK3CA* allele, only the wild-type protein was expressed, resulting in lower PI3K activity (labeled Wild-Type). This was confirmed by assessing the level of AKT and PRAS40 phosphorylation in the isogenic cells (Figure 3*A*). HCT116 and DLD-1 cells that only expressed wild-type *PIK3CA* (low PI3K activity) were significantly more sensitive to ABT-737 than corresponding parental cells (Figure 3*B* and Table W2). HCT116 cells that only expressed mutant *PIK3CA* (high PI3K activity) were significantly more resistant to ABT-737 than HCT116 parental cells, and DLD-1 cells with mutant *PIK3CA* were as resistant as parental cells. These data demonstrate that reduced PI3K activity correlates with increased ABT-737 sensitivity, suggesting that the observed effect of PI-103 was not due to off-target effects. However, as both targets of PI-103 are components of the PI3K signaling pathway, it remained unclear which target of PI-103 was responsible for the enhanced ABT-737 sensitivity. To investigate this further, the effect of a panel of PI3K pathway inhibitors on ABT-737 sensitivity was assessed in HCT116 and SW620 cells, specifically GDC-0941, a class I PI3K-specific inhibitor [28], rapamycin, an mTOR complex 1 (mTORC1)-specific inhibitor [29], KU-0063794, an ATP-competitive mTOR inhibitor that inhibits mTORC1 and mTORC2 but not PI3K [30], and AKTi1/2 and MK-2206, two allosteric AKT inhibitors [31,32]. All agents were used at concentrations that demonstrably inhibited their primary targets: GDC-0941 and KU-0063794 inhibited phosphorylation of AKT, PRAS40, and S6; rapamycin inhibited S6 phosphorylation but increased AKT and PRAS40 phosphorylation; and AKTi1/2 and MK-2206 inhibited AKT and PRAS40 but not S6 phosphorylation (Figure 3*C*). In HCT116 and SW620 cells, GDC-0941 significantly sensitized to ABT-737, whereas rapamycin and KU-0063794 were without effect (Figure 3*D* and Table 2), suggesting that PI3K inhibition, rather than mTORC1/2 inhibition, was responsible for ABT-737 sensitization. Contrary to expectations, KU-0063794 did not sensitize to ABT-737 despite the fact that AKT is a target of mTORC2 (Figure 3*C*) and AKT is considered the main downstream effector of PI3K [6]. To explore this further, the effect of AKT inhibition on ABT-737 sensitivity was investigated. In both cell lines, neither AKTi1/2 nor MK-2206 had a significant effect on the sensitivity to ABT-737 (Figure 3*D* and Table 2), strongly suggesting that the downstream target of PI3K responsible for ABT-737 sensitization is AKT independent and implicating a novel, antiapoptotic PI3K-dependent, AKT-independent signaling pathway. The ABT-737 concentration-response data were verified by combining ABT-737 with each of the PI3K pathway inhibitors and monitoring caspase activation in SW620 cells (Figure 3*E*). Only PI-103 and GDC-0941 when combined with ABT-737 caused a significant increase in the number of cells with activated caspase compared to ABT-737 alone, consistent with the ABT-737 concentration-response data. Furthermore, the PI-103–induced down-regulation of MCL-1 was not observed with Akti1/2 or rapamycin treatment (Figure W4), and neither Akti1/2 nor rapamycin was able to further sensitize MCL-1–depleted SW620 cells to ABT-737 (Figure W5 and Table W3). These data are consistent with at least two antiapoptotic AKT/mTOR-independent pathways acting downstream of PI3K, only one of which affects MCL-1 levels.

BMX Down-Regulation Sensitized to ABT-737

The secondary messenger generated by class I PI3K, PtdIns(3,4,5)P_3, has the potential to regulate many proteins in addition to AKT. Indeed, there are reported to be >50 proteins that can bind to PtdIns(3,4,5)P_3 [3]. To determine whether any of these proteins may be involved in the PI3K inhibition–induced sensitization to ABT-737, a SMARTpool siRNA library targeting mRNA for each of 52 proteins containing a PH domain that interacts with PtdIns(3,4,5)P_3 and other core PI3K pathway proteins was designed (Table W4). SW620 cells, which exhibited the greatest degree of sensitization to ABT-737 when PI3K signaling was inhibited, were transfected with each siRNA, and the effect of ABT-737 treatment determined relative to nontargeting siRNA–transfected cells (Figure 4*A*, *left panel*). Four siRNAs were shown to induce a significant ($P < .05$; robust z score < –0.9) increase in ABT-737 sensitivity (Figure 4*A*, *right panel*, and Table W4). Of these four siRNAs, BMX, SOS1, and SGK1 were chosen for further analysis. A complete ABT-737 concentration response was carried out on cells transfected with each of the individual siRNA oligos that made up the SMARTpool with some oligos demonstrating a degree of sensitization for all three targets (Figures 4*B* and W6). However, only oligos 1 and 3 targeting BMX produced a significant sensitization to ABT-737 ($P = .041$ and .022, respectively; Table W5). Furthermore, when the association between the level of mRNA knockdown for each oligo set and the sensitization toward ABT-737 was assessed, only knockdown of BMX significantly correlated with ABT-737 efficacy ($P = .0015$; Figures 4*C* and W6*B*). The BMX siRNA oligos that gave the greatest degree of ABT-737 sensitization, SMARTpool, oligos 1 and 3, also caused the greatest reduction of BMX protein expression (Figure W7). BMX knockdown in HCT116 cells also sensitized to ABT-737 (Figure 4*D* and Table W6). Moreover, pharmacological inhibition of BMX with the TEC family

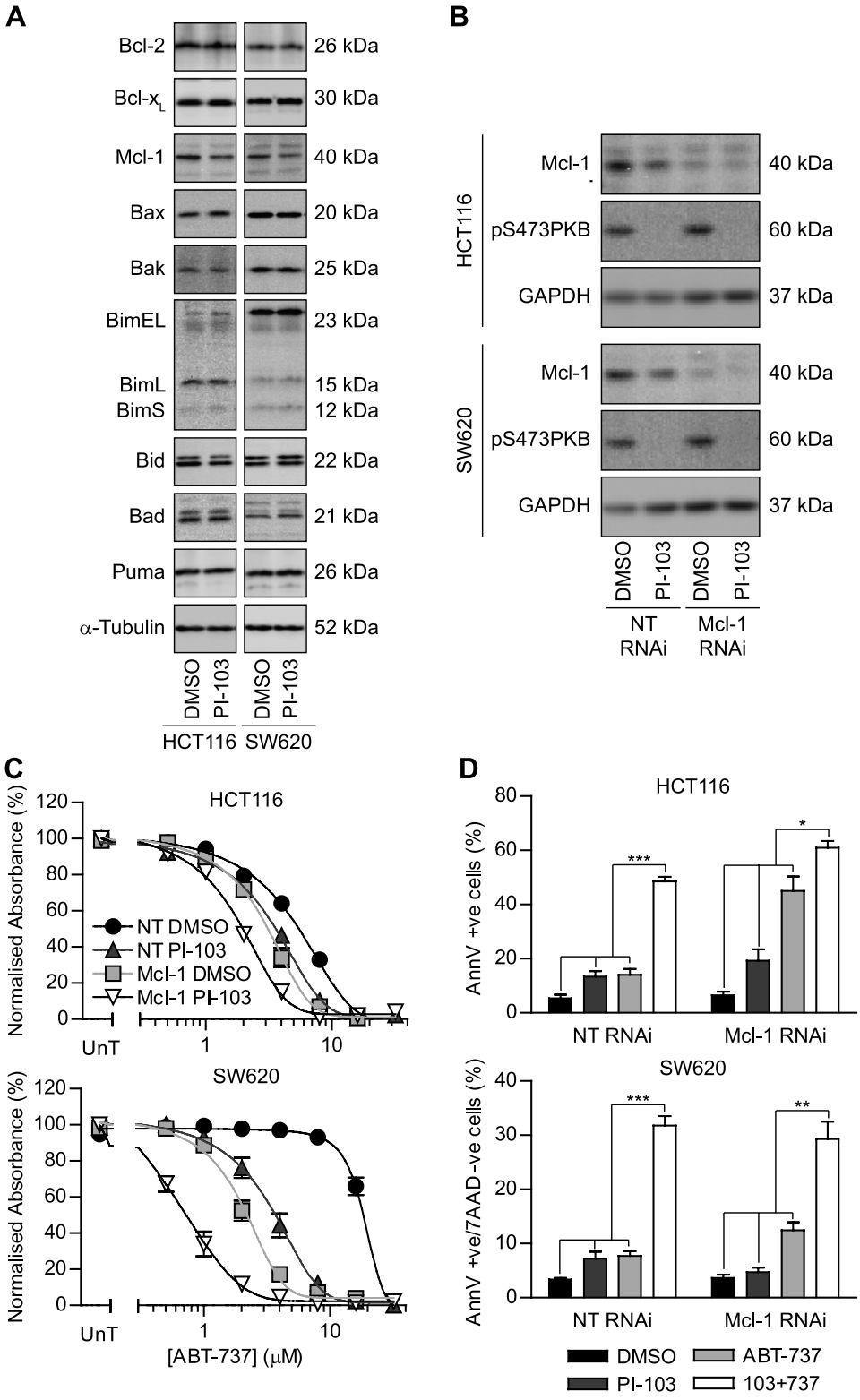

Figure 2. Reduced MCL-1 level is not solely responsible for increased ABT-737 sensitivity. (A) HCT116 and SW620 cells were treated with DMSO equivalent or 2 μM PI-103 for 24 hours, and the level of Bcl-2, BCL-XL, MCL-1, Bax, Bak, Bim, Bid, Puma, Bad, and Noxa was determined by Western blot analysis. (B–D) HCT116 and SW620 cells were transfected with nontargeting siRNA (NT RNAi) or siRNA targeting MCL-1 (MCL-1 RNAi) and plated for experiments 24 hours later. Cells were treated with 2 μM PI-103 for 24 hours, and the effect on levels of MCL-1, pS473 AKT, and GAPDH was determined by Western blot analysis (B). RNAi cells were treated with 2 μM PI-103 or DMSO equivalent and the indicated concentration of ABT-737 for 3 days and processed as in Figure 1*A* (C). RNAi cells were treated with 2 μM PI-103 and/or 4 μM ABT-737 (NT RNAi), 2 μM ABT-737 (HCT116 MCL-1 RNAi), or 1 μM ABT-737 (SW620 MCL-1 RNAi) for 24 hours. Cells were stained with APC-conjugated annexin V and 7AAD and analyzed by flow cytometry (D). All blots are representative of three independent experiments, and all graphs represent the means of three independent experiments carried out in triplicate (C) or duplicate (D) ± SEM. *$P < .05$, **$P < .01$, and ***$P < .001$ according to two-tailed unpaired *t* test.

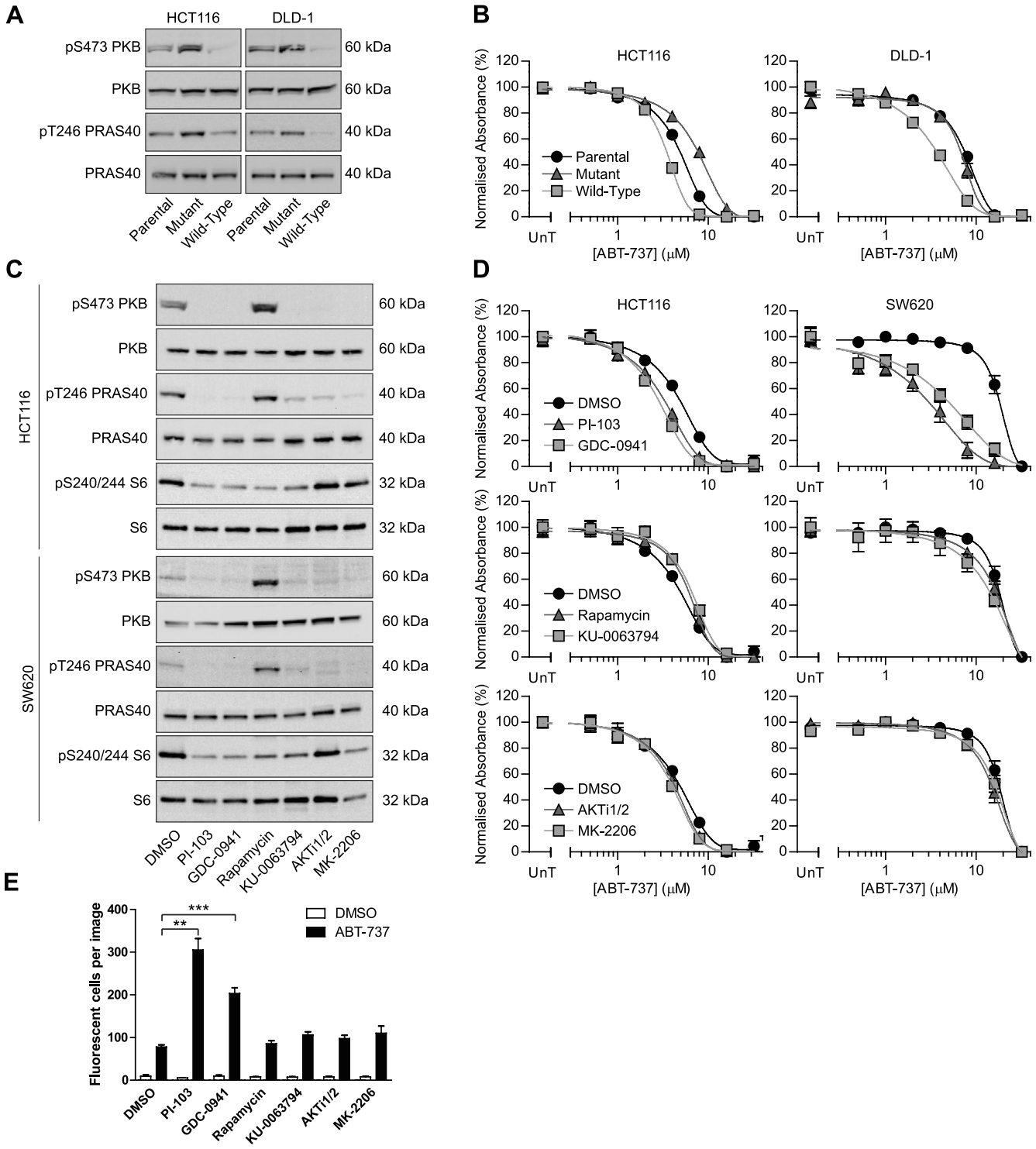

Figure 3. ABT-737 sensitization was PI3K dependent but AKT and mTOR independent. (A and B) Parental HCT116 and DLD-1 cells or cells expressing only the mutant or wild-type *PIK3CA* allele were assessed for the level of pS473 AKT, total AKT, pT246 PRAS40, or total PRAS40 by Western blot analysis (A) or exposed to the indicated concentrations of ABT-737 and processed as in Figure 1*A* (B). (C) HCT116 and SW620 cells were exposed to 2 μM PI-103, 2 μM GDC-0941, 10 nM rapamycin, 2 μM KU-0063794, 1 μM AKTi1/2, or 1 μM MK-2206 for 4 hours, and the effect on level of pS473 AKT, total AKT, pT246 PRAS40, total PRAS40, pS240/244 S6, and total S6 was determined by Western blot analysis. (D) HCT116 and SW620 cells were treated with the same concentrations of PI3K pathway inhibitors as in C and the indicated concentrations of ABT-737 for 3 days and processed as in Figure 1*A*. (E) SW620 cells were treated with the same concentrations of PI3K pathway inhibitors as in C with or without 4 μM ABT-737 plus CellPlayer Caspase 3/7 reagent, which fluoresces after cleavage by caspases. Number of fluorescent cells was determined 8 hours after start of treatment. All blots are representative of three independent experiments, and all graphs represent the means of three independent experiments carried out in triplicate (B and D) or duplicate (E) ± SEM. $^{**}P < .01$ and $^{***}P < .001$ according to two-tailed unpaired *t* test.

Table 2. Effect of PI3K Pathway Inhibitors on ABT-737 GI_{50}.

Cell Line	Treatment	ABT-737 GI_{50} (μM ± 95% CI)	Significance*
HCT116	DMSO	4.95 (4.15-5.90)	
	2 μM PI-103	3.33 (2.88-3.84)	0.0268
	2 μM GDC0941	2.73 (2.54-2.93)	0.0036
	1 μM AKTi1/2	4.32 (4.17-4.46)	0.2092
	1 μM MK2206	4.06 (3.72-4.43)	0.1189
	10 nM rapamycin	6.19 (5.77-6.64)	0.0821
	2 μM KU0063794	6.57 (6.10-7.07)	0.0441
SW620	DMSO	16.9 (15.4-18.5)	
	2 μM PI-103	3.15 (2.45-4.05)	0.0002
	2 μM GDC0941	6.09 (3.10-11.9)	0.0424
	1 μM AKTi1/2	14.5 (11.4-18.5)	0.3140
	1 μM MK2206	20.0 (10.6-37.6)	0.6317
	10 nM rapamycin	15.3 (12.8-18.4)	0.4049
	2 μM KU0063794	16.4 (12.9-20.8)	0.8369

*Two-tailed unpaired *t* test *versus* DMSO-treated GI_{50} for same cell line.

kinase inhibitor PCI-32765 (ibrutinib [33]) in SW620, HCT116, and DLD-1 cells sensitized to ABT-737 (Figures 4*E* and W8, and Table W7). To determine whether BMX acted downstream of PI3K with regard to ABT-737 sensitization, the effect of BMX knockdown and PI-103 treatment on ABT-737 sensitivity was assessed. Knockdown of BMX did not further sensitize PI-103–treated SW620 cells to ABT-737 (Figure 4*F* and Table W8), suggesting that BMX-induced sensitization to ABT-737 is downstream of PI3K. BMX inhibition, either by RNAi or treatment with PCI-32765, did not affect expression of MCL-1 (Figure W9), suggesting that sensitization to ABT-737 is through an MCL-1–independent mechanism. Together, these data suggest that inhibition of BMX activity, either through knockdown or pharmacological inhibition, can sensitize CRC cell lines to ABT-737. This indicates that this PH domain–containing protein may represent a key AKT-independent effector downstream of PI3K that is responsible for PI3K inhibition–induced ABT-737 sensitization.

Discussion

In this study, we presented evidence that the inhibition of PI3K signaling increased the sensitivity of CRC cells to ABT-737–induced apoptosis. This effect was shown to be independent of AKT inhibition and in part due to factors additional to the observed MCL-1 down-regulation. Furthermore, we present data demonstrating that inhibition of the TEC kinase BMX also sensitizes to ABT-737. This raises the possibility that BMX is a key downstream target of PI3K signaling mediating ABT-737 sensitivity and suggests that the PI3K/BMX axis may have antiapoptotic activity in CRC cells.

Other studies in non–small cell lung cancer [18] and lymphoma cell lines [17] have demonstrated that canonical PI3K pathway inhibition downstream of PI3K increased apoptosis in response to ABT-737 (or navitoclax). BCL-XL prevented PI3K inhibition–induced apoptosis in non–small cell lung cancer cells, and this was overcome by ABT-737; however, PI3K inhibition was phenocopied in AKT-depleted cells, suggesting that the antiapoptotic effect of PI3K signaling was AKT dependent [18]. Rapamycin increased navitoclax-induced apoptosis in lymphoma cells *in vitro* and *in vivo*, although the mechanism of action was not investigated [17]. Taken together, these three studies suggest that there are different mechanisms downstream of PI3K signaling to suppress ABT-737–induced apoptosis and that these mechanisms are context dependent. In support of this, a study investigating the importance of AKT in cellular proliferation/survival across a panel of human tumor cell lines revealed that a subset of cell lines (including HCT116 and DLD-1) was dependent on PI3K but not on AKT for proliferation and survival [34]. The lack of an absolute requirement for AKT in CRC cells has also been reported. When either *PDK1* or *AKT1* and *AKT2* were knocked out in both HCT116 and DLD-1 cells [35], the cells were able to survive in standard culture conditions. However, inhibition of PI3K signaling by pharmacological intervention or expression of a dominant negative PI3K subunit in the same cell lines ([7] and Figure W2) caused a profound proliferation delay. Overall, there are clearly cell line–dependent differences in signaling downstream of PI3K, and this emphasizes the need to broaden our understanding of this important signaling pathway beyond AKT and its known downstream targets.

The TEC family of kinases is the second largest family of nonreceptor protein tyrosine kinases, comprising five members, namely, TEC, BTK, ITK, TXK, and BMX (also known as ETK). Whereas TEC kinases are primarily expressed in hematopoietic cells, BMX and TEC have a broader expression profile. Specifically, BMX is expressed in endothelial linages as well as epithelial cancers such as breast and prostate [36]. All TEC kinases except TXK have a PH domain that interacts with PtdIns(3,4,5)P_3 and can be activated by PI3K signaling [37–39]. Furthermore, BMX has recently been implicated in mutant PIK3CA transformation [40]. BMX has been suggested to have an antiapoptotic function in prostate cancer cell lines [41], where expression of dominant negative BMX enhances chemotherapy- and radiotherapy-induced apoptosis. The downstream targets of BMX are not fully elucidated; although research has demonstrated that BMX can activate STAT3 [42] and also bind to and activate PAK1 [43], whether these targets are responsible for the antiapoptotic effect of BMX is unclear. BMX has been reported to bind to BCL-XL in bladder cancer cell lines [44], although the functional consequences of this interaction and how it is regulated have not been investigated. In the study reported here, we were unable to detect any change in phosphorylation of STAT proteins after treatment with PI3K or TEC kinase inhibitors (data not shown), and further investigation is now required to understand the antiapoptotic role of BMX in CRC better.

In addition to BMX, the RNAi library screen identified three other potential sensitizers to ABT-737, namely, SOS1, SGK1, and PLEKHB2. Further study with deconvolved SMARTpool siRNA oligos (Figures 4*C* and W5) suggested that the efficacy of SOS1 and SGK1 RNAi was probably due to off-target effects of some of the oligos, rather than knockdown of the intended target. PLEKHB2 was not investigated further as PLEKHB2's PH domain has recently been suggested to bind preferentially to phosphatidylserine rather than PtdIns(3,4,5)P_3 [45], and therefore, it is unlikely that PLEKHB2 is a downstream target of PI3K signaling. It is also interesting to note that knockdown of two PI3K subunits, PIK3CB and PIK3R1, was implicated in causing resistance to ABT-737 (Figure 4*A*). One possibility is that down-regulation of specific PI3K subunits (e.g., PIK3CB) leads to a compensatory up-regulation of other subunits (e.g., PIK3CA), and it is the upregulated subunit that drives ABT-737 resistance, a hypothesis that will be tested in future studies.

From a clinical perspective, the data presented here suggest that combining navitoclax with PI3K inhibitors or TEC kinase inhibitors may prove beneficial to patients with metastatic CRC, a population of patients with a 6% chance of 5-year survival (Colorectal Cancer Survival by Stage—NCIN Data Briefing 2009, http://tinyurl.com/pf5hl45), exemplifying the clinical need for improved therapy.

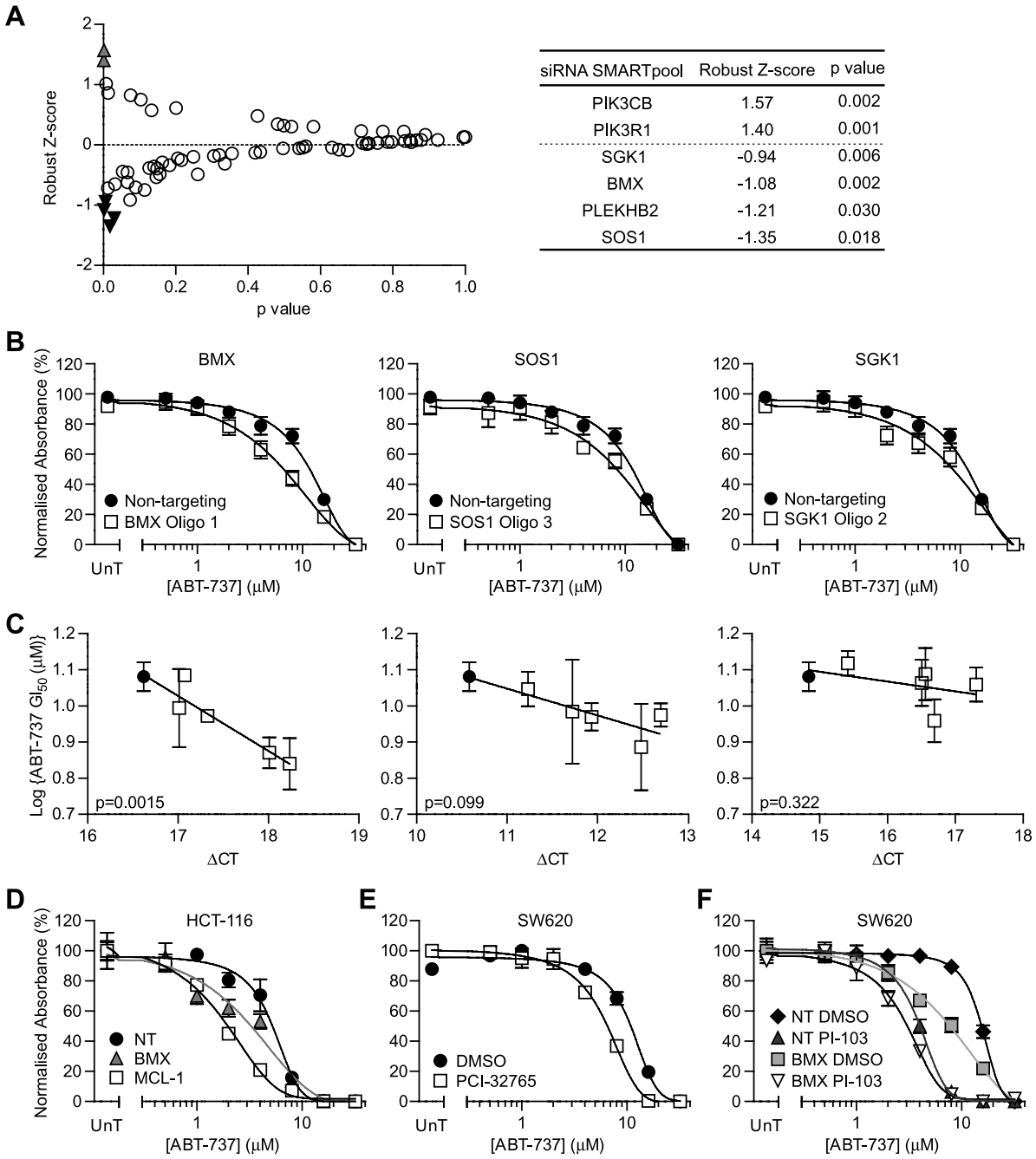

siRNA SMARTpool	Robust Z-score	p value
PIK3CB	1.57	0.002
PIK3R1	1.40	0.001
SGK1	-0.94	0.006
BMX	-1.08	0.002
PLEKHB2	-1.21	0.030
SOS1	-1.35	0.018

Figure 4. BMX knockdown and inhibition sensitized to ABT-737. (A) SW620 cells were transfected with an siRNA SMARTpool targeting 1 of 65 mRNA that encode proteins potentially involved in PI3K signaling or a nontargeting control. Forty-eight hours later, cells were treated with 4 μM ABT-737 or DMSO equivalent for 72 hours, and cellular biomass was determined by SRB staining. Robust *z* score of ABT-737–treated cells compared to DMSO control cells was calculated, and the *P* value for each SMARTpool compared to nontargeting control was determined by two-tailed unpaired *t* test. Values for SMARTpool that induce ABT-737 resistance (▲) and sensitivity (▼) are shown in right-hand table. (B and C) SW620 cells were transfected with nontargeting siRNA (●), SMARTpool siRNA, or individual oligos targeting BMX, SOS1, or SGK1 (□), and an ABT-737 concentration response was carried out, or the appropriate mRNA level was determined by qPCR. B shows the concentration response curve for the most effective siRNA oligo, and C shows the correlation between knockdown efficiency and ABT-737 efficacy. (D) HCT116 cells were transfected with nontargeting siRNA, BMX siRNA, or MCL-1 siRNA and the indicated concentration of ABT-737 for 3 days and processed as in Figure 1*A*. (E) SW620 cells were treated with 4 μM PCI-32765 or DMSO equivalent and the indicated concentration of ABT-737 for 3 days and processed as in Figure 1*A*. (F) SW620 cells were transfected with nontargeting siRNA or BMX oligo 1, treated with 2 μM PI-103 or DMSO equivalent and the indicated concentration of ABT-737 for 3 days, and processed as in Figure 1*A*. All graphs represent the means of three independent experiments carried out in triplicate ± SEM.

However, more research is needed to identify phenotypic and/or genotypic traits that predict for combinatorial efficacy. The data presented here demonstrate that PI3K inhibition increased apoptosis induced by ABT-737 more in SW620 cells (*PIK3CA* wild type) than in DLD-1 or HCT116 cells (*PIK3CA* mutant). However, we lack sufficient statistical power to conclude that these differences are due to *PIK3CA* status due to the plethora of other genetic differences between the cell lines. Therefore, to develop predictive biomarkers for this drug combination expansion to a larger panel of CRC cell lines with known genetic aberrations is required.

Acknowledgments

The authors thank John Brognard for advice on data interpretation and manuscript preparation and Becky Bola and Matthew Lancashire for editorial advice.

References

[1] FDA (2011). Regulatory watch: FDA guidance on co-developing investigational drugs. *Nat Rev Drug Discov* **10**, 86.

[2] Hanahan D and Weinberg RA (2011). Hallmarks of cancer: the next generation. *Cell* **144**, 646–674.

[3] Stephens L and Hawkins P (2010). Signalling via class IA PI3Ks. *Adv Enzyme Regul* **51**, 27–36.

[4] Vivanco I and Sawyers CL (2002). The phosphatidylinositol 3-kinase–AKT pathway in human cancer. *Nat Rev Cancer* **2**, 489–501.

[5] Manning BD and Cantley LC (2007). AKT/PKB signaling: navigating downstream. *Cell* **129**, 1261–1274.

[6] Engelman JA (2009). Targeting PI3K signalling in cancer: opportunities, challenges and limitations. *Nat Rev Cancer* **9**, 550–562.

[7] Martin-Fernandez C, Bales J, Hodgkinson C, Welman A, Welham MJ, Dive C, and Morrow CJ (2009). Blocking phosphoinositide 3-kinase activity in colorectal cancer cells reduces proliferation but does not increase apoptosis alone or in combination with cytotoxic drugs. *Mol Cancer Res* **7**, 955–965.

[8] Raynaud FI, Eccles S, Clarke PA, Hayes A, Nutley B, Alix S, Henley A, Di-Stefano F, Ahmad Z, Guillard S, et al. (2007). Pharmacologic characterization of a potent inhibitor of class I phosphatidylinositide 3-kinases. *Cancer Res* **67**, 5840–5850.

[9] Guillard S, Clarke PA, Te Poele R, Mohri Z, Bjerke L, Valenti M, Raynaud F, Eccles SA, and Workman P (2009). Molecular pharmacology of phosphatidylinositol 3-kinase inhibition in human glioma. *Cell Cycle* **8**, 443–453.

[10] Opel D, Westhoff MA, Bender A, Braun V, Debatin KM, and Fulda S (2008). Phosphatidylinositol 3-kinase inhibition broadly sensitizes glioblastoma cells to death receptor– and drug-induced apoptosis. *Cancer Res* **68**, 6271–6280.

[11] Chonghaile TN and Letai A (2008). Mimicking the BH3 domain to kill cancer cells. *Oncogene* **27**(suppl 1), S149–S157.

[12] Oltersdorf T, Elmore SW, Shoemaker AR, Armstrong RC, Augeri DJ, Belli BA, Bruncko M, Deckwerth TL, Dinges J, Hajduk PJ, et al. (2005). An inhibitor of Bcl-2 family proteins induces regression of solid tumours. *Nature* **435**, 677–681.

[13] Del Gaizo Moore V, Schlis KD, Sallan SE, Armstrong SA, and Letai A (2008). BCL-2 dependence and ABT-737 sensitivity in acute lymphoblastic leukemia. *Blood* **111**, 2300–2309.

[14] Wilson WH, O'Connor OA, Czuczman MS, LaCasce AS, Gerecitano JF, Leonard JP, Tulpule A, Dunleavy K, Xiong H, Chiu YL, et al. (2010). Navitoclax, a targeted high-affinity inhibitor of BCL-2, in lymphoid malignancies: a phase 1 dose-escalation study of safety, pharmacokinetics, pharmacodynamics, and antitumour activity. *Lancet Oncol* **11**, 1149–1159.

[15] Harrison LR, Micha D, Brandenburg M, Simpson KL, Morrow CJ, Denneny O, Hodgkinson C, Yunus Z, Dempsey C, Roberts D, et al. (2011). Hypoxic human cancer cells are sensitized to BH-3 mimetic-induced apoptosis via downregulation of the Bcl-2 protein Mcl-1. *J Clin Invest* **121**, 1075–1087.

[16] Cragg MS, Harris C, Strasser A, and Scott CL (2009). Unleashing the power of inhibitors of oncogenic kinases through BH3 mimetics. *Nat Rev Cancer* **9**, 321–326.

[17] Ackler S, Xiao Y, Mitten MJ, Foster K, Oleksijew A, Refici M, Schlessinger S, Wang B, Chemburkar SR, Bauch J, et al. (2008). ABT-263 and rapamycin act cooperatively to kill lymphoma cells *in vitro* and *in vivo*. *Mol Cancer Ther* **7**, 3265–3274.

[18] Qian J, Zou Y, Rahman JS, Lu B, and Massion PP (2009). Synergy between phosphatidylinositol 3-kinase/Akt pathway and Bcl-xL in the control of apoptosis in adenocarcinoma cells of the lung. *Mol Cancer Ther* **8**, 101–109.

[19] Klymenko T, Brandenburg M, Morrow C, Dive C, and Makin G (2011). The novel Bcl-2 inhibitor ABT-737 is more effective in hypoxia and is able to reverse hypoxia-induced drug resistance in neuroblastoma cells. *Mol Cancer Ther* **10**, 2373–2383.

[20] Morrow CJ, Gray A, and Dive C (2005). Comparison of phosphatidylinositol-3-kinase signalling within a panel of human colorectal cancer cell lines with mutant or wild-type PIK3CA. *FEBS Lett* **579**, 5123–5128.

[21] Cardone MH, Roy N, Stennicke HR, Salvesen GS, Franke TF, Stanbridge E, Frisch S, and Reed JC (1998). Regulation of cell death protease caspase-9 by phosphorylation. *Science* **282**, 1318–1321.

[22] Datta SR, Dudek H, Tao X, Masters S, Fu H, Gotoh Y, and Greenberg ME (1997). Akt phosphorylation of BAD couples survival signals to the cell-intrinsic death machinery. *Cell* **91**, 231–241.

[23] Griffiths GJ, Dubrez L, Morgan CP, Jones NA, Whitehouse J, Corfe BM, Dive C, and Hickman JA (1999). Cell damage-induced conformational changes of the pro-apoptotic protein Bak *in vivo* precede the onset of apoptosis. *J Cell Biol* **144**, 903–914.

[24] Konopleva M, Contractor R, Tsao T, Samudio I, Ruvolo PP, Kitada S, Deng X, Zhai D, Shi YX, Sneed T, et al. (2006). Mechanisms of apoptosis sensitivity and resistance to the BH3 mimetic ABT-737 in acute myeloid leukemia. *Cancer Cell* **10**, 375–388.

[25] van Delft MF, Wei AH, Mason KD, Vandenberg CJ, Chen L, Czabotar PE, Willis SN, Scott CL, Day CL, Cory S, et al. (2006). The BH3 mimetic ABT-737 targets selective Bcl-2 proteins and efficiently induces apoptosis via Bak/Bax if Mcl-1 is neutralized. *Cancer Cell* **10**, 389–399.

[26] Faber AC, Li D, Song Y, Liang MC, Yeap BY, Bronson RT, Lifshits E, Chen Z, Maira SM, Garcia-Echeverria C, et al. (2009). Differential induction of apoptosis in HER2 and EGFR addicted cancers following PI3K inhibition. *Proc Natl Acad Sci USA* **106**, 19503–19508.

[27] Samuels Y, Diaz LA Jr, Schmidt-Kittler O, Cummins JM, Delong L, Cheong I, Rago C, Huso DL, Lengauer C, Kinzler KW, et al. (2005). Mutant PIK3CA promotes cell growth and invasion of human cancer cells. *Cancer Cell* **7**, 561–573.

[28] Folkes AJ, Ahmadi K, Alderton WK, Alix S, Baker SJ, Box G, Chuckowree IS, Clarke PA, Depledge P, Eccles SA, et al. (2008). The identification of 2-(1H-indazol-4-yl)-6-(4-methanesulfonyl-piperazin-1-ylmethyl)-4-morpholin-4-yl-thieno[3,2-d]pyrimidine (GDC-0941) as a potent, selective, orally bioavailable inhibitor of class I PI3 kinase for the treatment of cancer. *J Med Chem* **51**, 5522–5532.

[29] Sarbassov DD, Ali SM, Kim DH, Guertin DA, Latek RR, Erdjument-Bromage H, Tempst P, and Sabatini DM (2004). Rictor, a novel binding partner of mTOR, defines a rapamycin-insensitive and raptor-independent pathway that regulates the cytoskeleton. *Curr Biol* **14**, 1296–1302.

[30] Garcia-Martinez JM, Moran J, Clarke RG, Gray A, Cosulich SC, Chresta CM, and Alessi DR (2009). Ku-0063794 is a specific inhibitor of the mammalian target of rapamycin (mTOR). *Biochem J* **421**, 29–42.

[31] Barnett SF, Defeo-Jones D, Fu S, Hancock PJ, Haskell KM, Jones RE, Kahana JA, Kral AM, Leander K, Lee LL, et al. (2005). Identification and characterization of pleckstrin-homology-domain-dependent and isoenzyme-specific Akt inhibitors. *Biochem J* **385**, 399–408.

[32] Hirai H, Sootome H, Nakatsuru Y, Miyama K, Taguchi S, Tsujioka K, Ueno Y, Hatch H, Majumder PK, Pan BS, et al. (2010). MK-2206, an allosteric Akt inhibitor, enhances antitumor efficacy by standard chemotherapeutic agents or molecular targeted drugs *in vitro* and *in vivo*. *Mol Cancer Ther* **9**, 1956–1967.

[33] Honigberg LA, Smith AM, Sirisawad M, Verner E, Loury D, Chang B, Li S, Pan Z, Thamm DH, Miller RA, et al. (2010). The Bruton tyrosine kinase inhibitor PCI-32765 blocks B-cell activation and is efficacious in models of autoimmune disease and B-cell malignancy. *Proc Natl Acad Sci USA* **107**, 13075–13080.

[34] Vasudevan KM, Barbie DA, Davies MA, Rabinovsky R, McNear CJ, Kim JJ, Hennessy BT, Tseng H, Pochanard P, Kim SY, et al. (2009). AKT-independent signaling downstream of oncogenic PIK3CA mutations in human cancer. *Cancer Cell* **16**, 21–32.

[35] Ericson K, Gan C, Cheong I, Rago C, Samuels Y, Velculescu VE, Kinzler KW, Huso DL, Vogelstein B, and Papadopoulos N (2010). Genetic inactivation of

AKT1, AKT2, and PDPK1 in human colorectal cancer cells clarifies their roles in tumor growth regulation. *Proc Natl Acad Sci USA* **107**, 2598–2603.

[36] Cenni B, Gutmann S, and Gottar-Guillier M (2012). BMX and its role in inflammation, cardiovascular disease, and cancer. *Int Rev Immunol* **31**, 166–173.

[37] August A, Sadra A, Dupont B, and Hanafusa H (1997). Src-induced activation of inducible T cell kinase (ITK) requires phosphatidylinositol 3-kinase activity and the Pleckstrin homology domain of inducible T cell kinase. *Proc Natl Acad Sci USA* **94**, 11227–11232.

[38] Li Z, Wahl MI, Eguinoa A, Stephens LR, Hawkins PT, and Witte ON (1997). Phosphatidylinositol 3-kinase-γ activates Bruton's tyrosine kinase in concert with Src family kinases. *Proc Natl Acad Sci USA* **94**, 13820–13825.

[39] Qiu Y, Robinson D, Pretlow TG, and Kung HJ (1998). Etk/Bmx, a tyrosine kinase with a pleckstrin-homology domain, is an effector of phosphatidylinositol 3′-kinase and is involved in interleukin 6-induced neuroendocrine differentiation of prostate cancer cells. *Proc Natl Acad Sci USA* **95**, 3644–3649.

[40] Hart JR, Liao L, Yates JR III, and Vogt PK (2011). Essential role of Stat3 in PI3K-induced oncogenic transformation. *Proc Natl Acad Sci USA* **108**, 13247–13252.

[41] Xue LY, Qiu Y, He J, Kung HJ, and Oleinick NL (1999). Etk/Bmx, a PH-domain containing tyrosine kinase, protects prostate cancer cells from apoptosis induced by photodynamic therapy or thapsigargin. *Oncogene* **18**, 3391–3398.

[42] Tsai YT, Su YH, Fang SS, Huang TN, Qiu Y, Jou YS, Shih HM, Kung HJ, and Chen RH (2000). Etk, a Btk family tyrosine kinase, mediates cellular transformation by linking Src to STAT3 activation. *Mol Cell Biol* **20**, 2043–2054.

[43] Bagheri-Yarmand R, Mandal M, Taludker AH, Wang RA, Vadlamudi RK, Kung HJ, and Kumar R (2001). Etk/Bmx tyrosine kinase activates Pak1 and regulates tumorigenicity of breast cancer cells. *J Biol Chem* **276**, 29403–29409.

[44] Guo S, Sun F, Guo Z, Li W, Alfano A, Chen H, Magyar CE, Huang J, Chai TC, Qiu S, et al. (2011). Tyrosine kinase ETK/BMX is up-regulated in bladder cancer and predicts poor prognosis in patients with cystectomy. *PLoS One* **6**, e17778.

[45] Uchida Y, Hasegawa J, Chinnapen D, Inoue T, Okazaki S, Kato R, Wakatsuki S, Misaki R, Koike M, Uchiyama Y, et al. (2011). Intracellular phosphatidylserine is essential for retrograde membrane traffic through endosomes. *Proc Natl Acad Sci USA* **108**, 15846–15851.

Supplemental Materials and Methods

Robust Z Score Calculation

Sensitivity to ABT-737 for each siRNA SMARTPool was assessed calculating the surviving fraction following treatment with 4 μM ABT-737 for 72 hours for each siRNA target. Surviving fraction = replicate well with ABT-737/(average of three replicate wells with DMSO). The robust *z* score was used to analyze siRNA screen data. Robust *z* score is the number of median absolute deviations (MADs); a value is from the median value of the data set. The robust *z* score is used because it reduces the effect of outliers on the results and prevents missing potential significant changes in sensitivity to ABT-737. First, the new surviving fractions are calculated. New surviving fraction = median surviving fraction for all 65 siRNAs – individual surviving fraction. Negative new surviving fractions are converted to positive values, and the MAD is then calculated. MAD = SD (new surviving fractions) × 1.4826. The robust *z* score for each replicate can be calculated. Robust *z* score = [(surviving fraction – median surviving fraction)/MAD] × 1.4826.

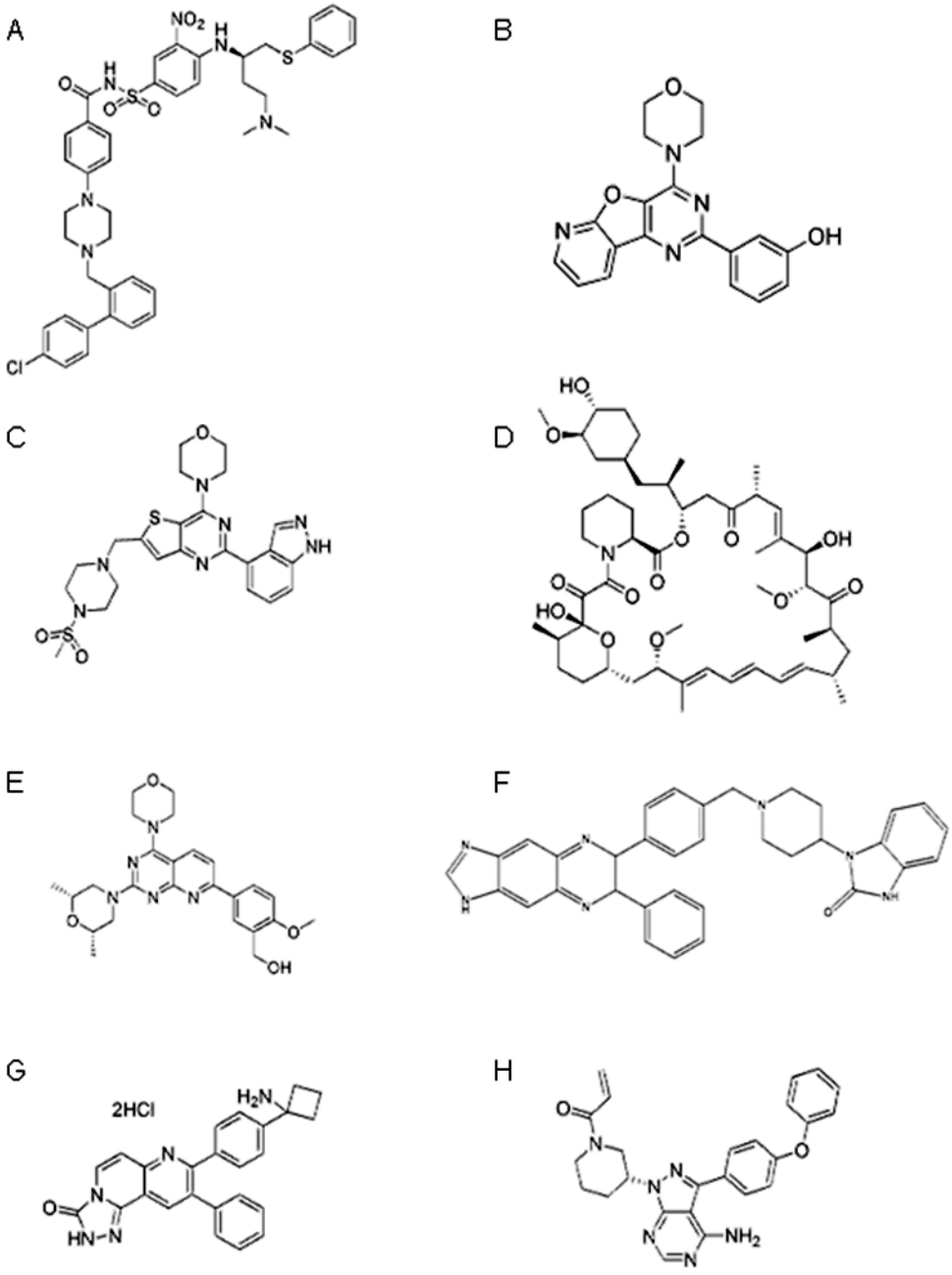

Figure W1. Structures of inhibitors used in study. (A) ABT-737, (B) PI-103, (C) GDC-0941, (D) rapamycin, (E) KU-0063794, (F) AKTi1/2, (G) MK-2206, and (H) PCI-32765.

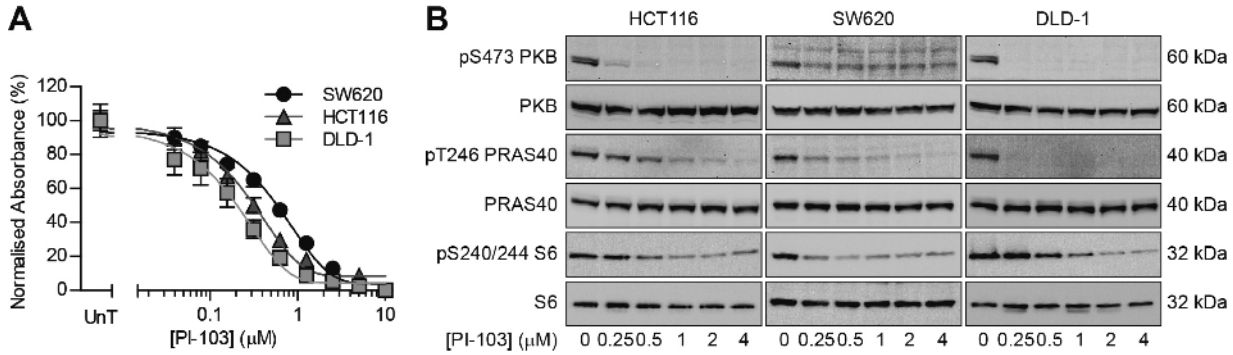

Figure W2. PI-103 inhibited cell proliferation and PI3K and mTOR signaling. (A) Cells were exposed to the indicated concentration of PI-103 for 3 days. Cells were fixed and stained with SRB, and the absorbance relative to untreated (UnT) cells was determined. Data represent the means of three independent experiments carried out in triplicate ± SEM. (B) Cells were exposed to the indicated concentration of PI-103 for 4 hours, and the effect on level of pS473 PKB, total PKB, pT246 PRAS40, total PRAS40, pS240/244 S6, and total S6 was determined by Western blot analysis. Results are representative of three independent experiments.

Table W1. Effect of MCL-1 RNAi on ABT-737 GI_{50}.

Cell Line	Treatment*	ABT-737 GI_{50} (μM ± 95% CI)	Significance†	
			vs NT DMSO	*vs* MCL-1 DMSO
HCT116	NT DMSO	5.83 (5.39-6.31)		
	NT PI-103	3.64 (3.20-4.15)	0.0037	
	MCL-1 DMSO	3.07 (2.59-3.65)	0.0027	
	MCL-1 PI-103	1.90 (1.75-2.06)	<0.0001	0.0079
SW620	NT DMSO	18.0 (17.1-19.0)		
	NT PI-103	3.54 (2.75-4.55)	0.0002	
	MCL-1 DMSO	2.09 (1.76-2.48)	<0.0001	
	MCL-1 PI-103	0.71 (0.56-0.92)	<0.0001	0.0022

The table relates to Figures 4*B*, *C*, and W6.

*Cells were transfected with either nontargeting siRNA (NT) or MCL-1 targeting siRNA (MCL-1). Cells were also treated with 2 μM PI-103 or a DMSO equivalent.

†Two-tailed unpaired *t* test *versus* indicated treatment for the same cell line.

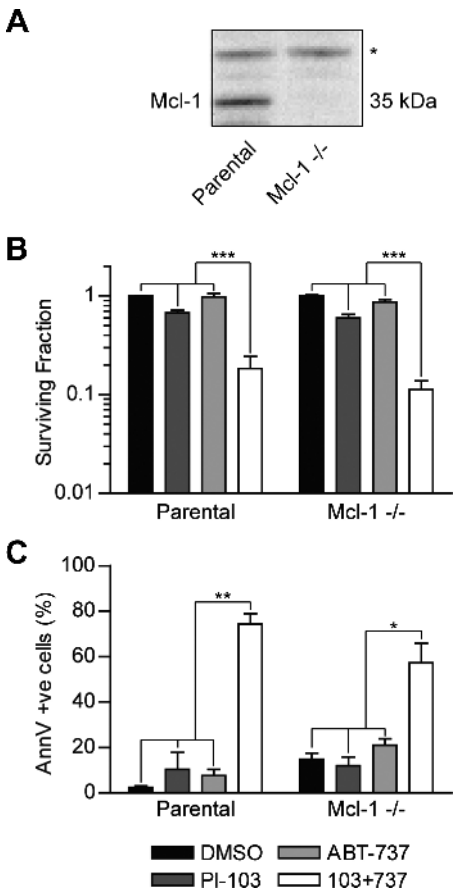

Figure W3. MCL-$1^{-/-}$ MEFs were sensitized to ABT-737–induced apoptosis by PI-103. (A) The level of MCL-1 in parental and MCL-$1^{-/-}$ MEFs was determined by Western blot analysis. *, nonspecific background band that acts as a loading control. (B) Parental and MCL-$1^{-/-}$ MEFs seeded at a low density were exposed to 2 μM PI-103 and/or 10 μM ABT-737 (parental) or 0.15 μM ABT-737 (MCL-$1^{-/-}$) for 3 days. Drugs were removed, and cells were left for 1 week for colonies to form. The number of colonies were counted and expressed as a surviving fraction relative to DMSO control. (C) Parental and MCL-$1^{-/-}$ MEFs were exposed to the same concentrations of PI-103 and ABT-737 as in B for 24 hours and stained with APC-conjugated annexin V. All graphs represent the means of three independent experiments carried out in duplicate ± SEM.

Table W2. Effect of PI3K Activity on ABT-737 GI_{50}.

Cell Line	PIK3CA Status	ABT-737 GI_{50} (μM ± 95% CI)	Significance*
HCT116	Parental	4.89 (4.55-5.24)	
	Mutant	8.16 (7.18-9.26)	0.0023
	Wild-type	3.40 (3.13-3.71)	0.0031
DLD-1	Parental	7.92 (7.29-8.61)	
	Mutant	6.97 (5.37-9.04)	0.4085
	Wild-type	3.76 (2.96-4.76)	0.0043

The table relates to Figure 3*B*.
*Two-tailed unpaired *t* test *versus* GI_{50} of parental cells for same cell line.

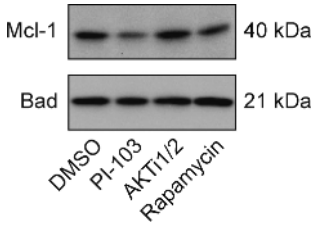

Figure W4. AKT and mTORC1 inhibition did not effect MCL-1 expression. HCT116 cells were treated with DMSO equivalent, 2 μM PI-103, 1 μM AKTi1/2, or 10 nM rapamycin for 24 hours, and the level of MCL-1 and Bad was determined by Western blot analysis.

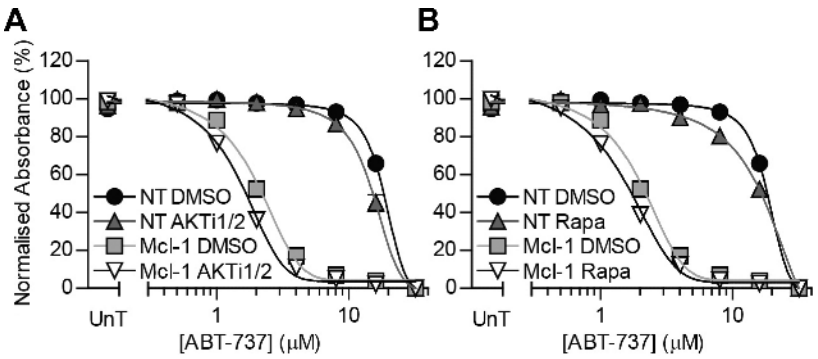

Figure W5. Neither AKTi1/2 nor rapamycin further sensitized MCL-1 knockdown SW620 cells to ABT-737. SW620 cells were transfected with NT RNAi or MCL-1 RNAi and plated for experiments 24 hours later. Cells were treated with 1 μM AKTi1/2 (A), 10 nM rapamycin (Rapa; B), or DMSO equivalent and the indicated concentration of ABT-737 for 3 days and processed as in Figure 1*A*. All graphs represent the means of three independent experiments carried out in triplicate ± SEM.

Table W3. Effect of MCL-1 RNAi on ABT-737 GI_{50}.

Cell Line	Treatment*	ABT-737 GI_{50} (μM ± 95% CI)	Significance†	
			vs NT DMSO	*vs* MCL-1 DMSO
SW620	NT DMSO	17.7 (17.3-18.2)		
	NT AKTi1/2	15.1 (13.0-17.7)	0.12	
	NT rapamycin	16.2 (14.5-18.1)	0.20	
	MCL-1 DMSO	2.1 (1.8-2.5)	<0.0001	
	MCL-1 AKTi1/2	1.6 (1.3-2.0)	<0.0001	0.11
	MCL-1 rapamycin	1.6 (1.3-2.1)	<0.0001	0.17

The table relates to Figure W5.
*Cells were transfected with either nontargeting siRNA (NT) or MCL-1 targeting siRNA (MCL-1). Cells were also treated with 1 μM AKTi1/2 or 10 nM rapamycin or a DMSO equivalent.
†Two-tailed unpaired *t* test *versus* indicated treatment for the same cell line.

Table W4. Results of siRNA Screen.

siRNA SMARTpool	Robust *Z* Score	*P* Value
MCL1	–4.669	4.66E-15
SOS1	–1.348	.018
PLEKHB2	–1.213	.030
BMX	–1.080	.002
SGK1	–0.944	.006
PIK3R2	–0.915	.074
AKT1	–0.746	.114
PHLDB3	–0.718	.013
PLEKHA2	–0.706	.089
SGK3	–0.649	.032
PIK3CD	–0.619	.067
AKT2	–0.535	.147
MCF2	–0.488	.261
DAPP1	–0.484	.156
FGD6	–0.456	.067
PREX2	–0.444	.054
ARAP3	–0.393	.149
VAV2	–0.382	.127
VAV1	–0.359	.140
ARHGEF4	–0.338	.183
DOCK1	–0.311	.336
GSK3B	–0.290	.163
PLEKHA1	–0.250	.216
TIAM1	–0.224	.206
PHLDB1	–0.197	.249
ADAP2	–0.186	.305
MTOR	–0.169	.320
GAB3	–0.141	.355
PIK3CA	–0.127	.419
ARAP1	–0.119	.434
SH3BP2	–0.079	.651
NT	–0.077	.539
SGK2	–0.056	.497
ARHGAP1	–0.055	.541
ADAP1	–0.045	.632
RASA2	–0.043	.552
VAV3	–0.025	.559
GSK3A	0.015	.726
SBF1	0.023	.733
PLCXD2	0.029	.732
CYTH4	0.031	.716
PLEK2	0.032	.758
ITK	0.046	.851
TEC	0.049	.796
PTPN9	0.067	.833
GAB1	0.078	.848
ARHGEF6	0.080	.865
SWAP70	0.083	.924
GAB2	0.084	.879
RASA3	0.131	.995
PREX1	0.167	.890
RICTOR	0.223	.830
PDPK1	0.224	.773
DOCK2	0.230	.712
CYTH2	0.301	.519
AKT3	0.303	.580
CYTH1	0.318	.498
ARAP2	0.345	.482
MYO10	0.482	.426
RASA1	0.572	.133
CYTH3	0.612	.201
BTK	0.751	.104
RPTOR	0.825	.075
AKAP13	0.861	.013
PLCL2	1.015	.008
PIK3R1	1.404	.001
PIK3CB	1.571	.002

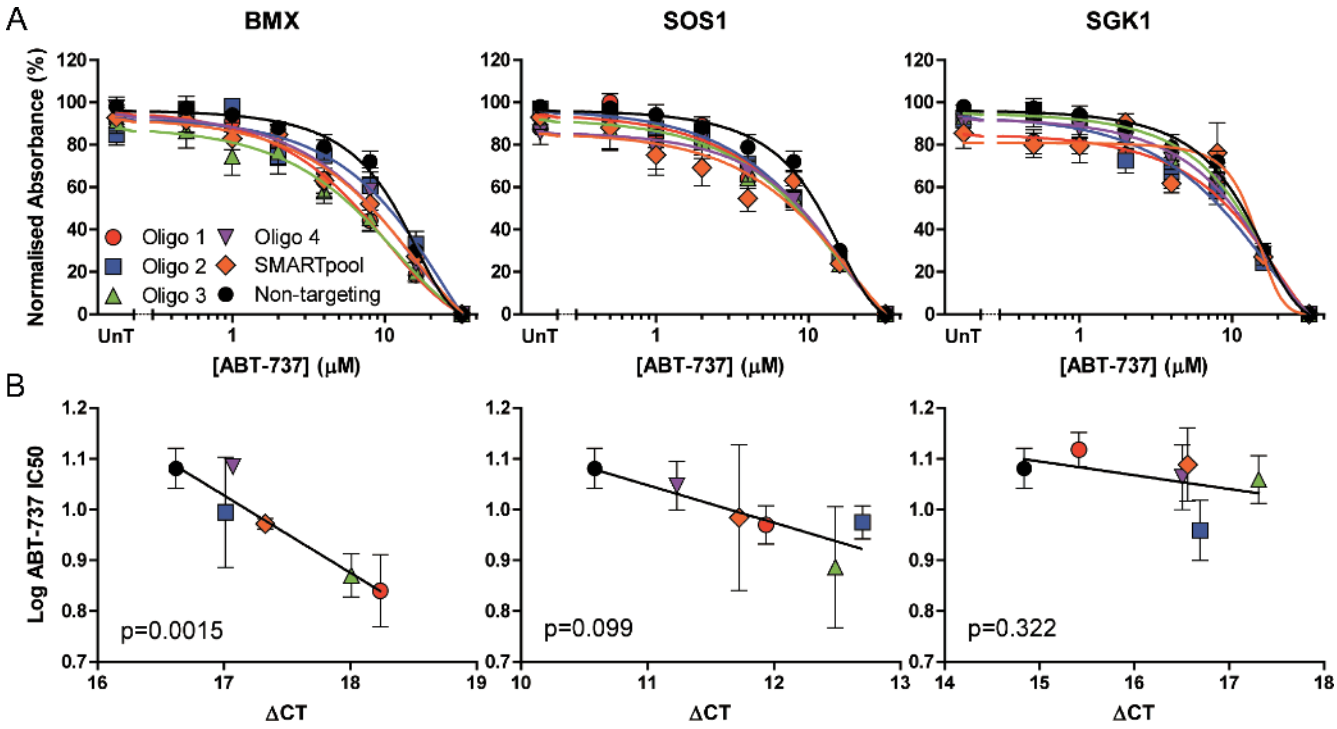

Figure W6. Deconvolution of BMX, SOS1, and SGK1 SMARTpool. SW620 cells were transfected with nontargeting siRNA, SMARTpool siRNA, or individual oligos targeting BMX, SOS1, or SGK1, and an ABT-737 concentration response was carried out, or the appropriate mRNA level was determined by qPCR. (A and B) A shows the concentration response curves, and B shows the correlation between knockdown efficiency and ABT-737 efficacy. All graphs represent the means of three independent experiments carried out in triplicate ± SEM.

Table W5. ABT-737 GI_{50} from Deconvolved siRNA Transfection.

RNAi Target	Oligo	ABT-737 GI_{50} (μM ± 95% CI)	Significance*
Nontargeting	SMARTpool	12.04 (10.07-14.10)	
BMX	1	6.92 (5.02-9.52)	0.041
	2	9.87 (6.06-16.08)	0.496
	3	7.42 (6.13-8.99)	0.022
	4	8.80 (4.68-16.56)	0.402
	SMARTpool	9.38 (8.95-9.83)	0.057
SOS1	1	9.33 (7.87-11.06)	0.113
	2	9.42 (8.16-10.91)	0.107
	3	7.70 (4.49-13.20)	0.198
	4	11.13 (8.98-13.81)	0.613
	SMARTpool	9.64 (5.04-18.44)	0.552
SGK1	1	13.11 (11.26-15.26)	0.516
	2	9.10 (6.96-11.89)	0.163
	3	11.46 (9.26-14.17)	0.744
	4	11.58 (8.69-15.44)	0.832
	SMARTpool	12.25 (8.85-16.96)	0.931

The table relates to Figures 4, *B* and *C*, and W4.
*Two-tailed unpaired *t* test *versus* nontargeting siRNA ABT-737 GI_{50}.

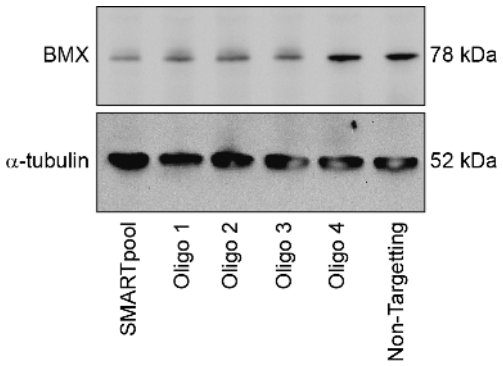

Figure W7. BMX RNAi reduced levels of BMX protein. SW620 cells were transfected with BMX siRNA SMARTpool, individual BMX siRNA oligos, or nontargeting control siRNA SMARTpool. After 48 hours, cells were harvested, and the level of BMX was assayed by Western blot analysis. Tubulin was used as a loading control. Blots are representative of three independent experiments.

Table W6. ABT-737 GI_{50} from HCT116 BMX RNAi.

RNAi Target	ABT-737 GI_{50} (μM ± 95% CI)	Significance*
Nontargeting	5.32 (4.40-6.43)	
BMX	2.94 (2.83-3.05)	0.027
MCL-1	1.70 (1.28-2.24)	0.022

The table relates to Figure 4*D*.
*Two-tailed unpaired *t* test *versus* nontargeting siRNA ABT-737 GI_{50}.

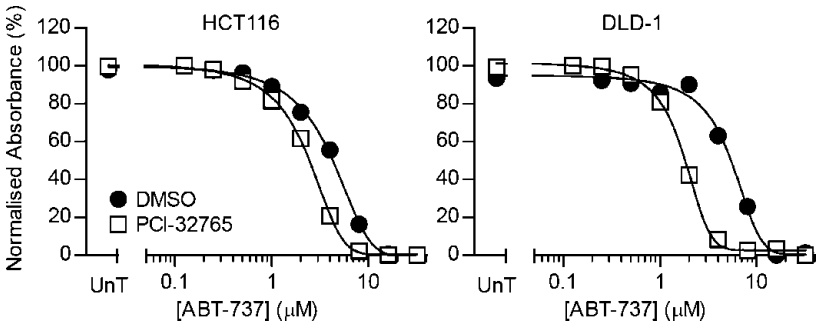

Figure W8. PCI-32765 increased the sensitivity of HCT116 and DLD-1 cells to ABT-737. HCT116 and DLD-1 cells were treated with 4 μM PCI-32765 or DMSO equivalent and the indicated concentration of ABT-737 for 3 days and processed as in Figure 1*A*. All graphs represent the means of three independent experiments carried out in triplicate. SEM error bars are not visible due to being smaller than the symbols.

Table W7. ABT-737 GI_{50} from SW620, HCT116 and DLD-1 PCI-32765 Treatment.

Cell Line	Treatment	ABT-737 GI_{50} (μM ± 95% CI)	Significance*
SW620	DMSO	10.8 (10.3-11.2)	
	4 μM PCI-32765	6.4 (5.9-6.9)	0.0005
HCT116	DMSO	4.2 (3.8-4.7)	
	4 μM PCI-32765	2.3 (2.0-2.7)	0.005
DLD-1	DMSO	5.4 (5.1-5.8)	
	4 μM PCI-32765	1.8 (1.7-1.8)	>0.0001

The table relates to Figures 4*E* and W8.
*Two-tailed unpaired *t* test *versus* nontargeting DMSO-treated ABT-737 GI_{50}.

Table W8. ABT-737 GI_{50} from SW620 BMX RNAi +/– PI-103.

Treatment*	ABT-737 GI_{50} (μM ± 95% CI)	Significance†	
		vs NT DMSO	*vs* NT PI-103
NT DMSO	15.4 (14.3-16.6)		
NT PI-103	3.79 (3.02-4.76)	0.0003	
BMX oligo 1 DMSO	8.0 (7.2-8.87)	0.0006	
BMX oligo 1 PI-103	2.93 (2.4-3.57)	0.0001	0.171

The table relates to Figure 4*F*.
*Cells were transfected with either nontargeting siRNA (NT) or BMX oligo 1. Cells were also treated with 2 μM PI-103 or a DMSO equivalent.
†Two-tailed unpaired *t* test *versus* indicated treatment for the same cell line.

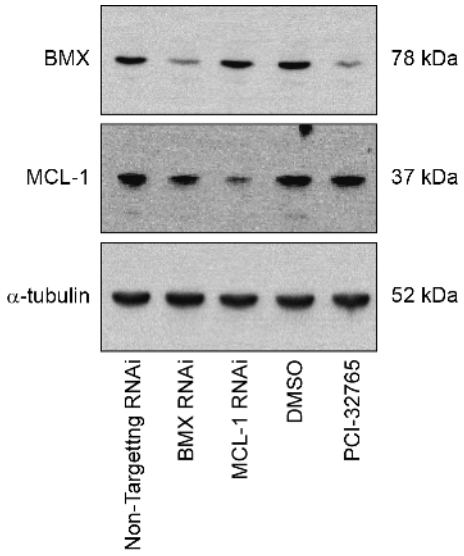

Figure W9. Neither BMX RNAi nor inhibition affected levels of MCL-1. SW620 cells were transfected with nontargeting siRNA, BMX siRNA, or MCL-1 siRNA SMARTpool and harvested 48 hours later to be treated with 4 μM PCI-32765 or DMSO equivalent and harvested 24 hours later. The level of BMX and MCL-1 was assayed by Western blot analysis. Tubulin was used as a loading control. Blots are representative of three independent experiments.